Antenna-Array Pattern Nulling Using a Differential Evolution Algorithm

Shiwen Yang, Yeow Beng Gan, Anyong Qing

Temasek Laboratories, National University of Singapore, EW2 #03-01, Engineering Drive 3, 10 Kent Ridge Crescent, Singapore 119260

Received 2 May 2003; accepted 13 August 2003

ABSTRACT: A new method based on the differential evolution (DE) algorithm is proposed for antenna-array pattern synthesis with prescribed nulls. The array excitation amplitudes are the only controlling parameters, and the objectives are to synthesize array patterns with nulls imposed on directions of interferences while keeping the sidelobe levels (SLLs) below prescribed levels. Many factors such as the excitation dynamic range ratio, null depth level, null width, and SLLs are taken into account in the synthesis. Simulation results of several typical problems are compared with published results to illustrate the effectiveness of the proposed method. © 2003 Wiley Periodicals, Inc. Int J RF and Microwave CAE 14: 57–63, 2004.

Keywords: antenna array; nulling; differential evolution

I. INTRODUCTION

Antenna-array pattern null forming and steering are very important in many electronic communication systems that function in strongly polluted electromagnetic environments. Methods of null steering, which have been studied extensively in the past, include controlling (i) the excitation amplitude and phase, (ii) the excitation amplitude only, (iii) the phase only, and (iv) the position only of the array elements. Each of the methods has its specific advantages and disadvantages. Generally, the null-steering problem is cast as an optimization problem, in which the excitation amplitudes, phases, and/or element positions are taken as the optimization parameters. The objectives then are to steer the nulls in the directions of interferences, while keeping the SLLs below certain levels. In terms of the search algorithms used for pattern nulling, many classical algorithms, such as the gradient search or steepest descent algorithm [1] and the minimax approximation method [2], are used. These classical algorithms usually need a starting point that is reasonably close to the final solution. Thus, they are extremely nearsighted and are usually trapped in a local minimum. In recent years, genetic algorithms (GAs) have been widely used in array-pattern nulling [3–7]. Compared to the classical algorithms, GAs use a population-based probabilistic search technique, which provides a mechanism for global searches and enables the ability to escape from local minima. However, GAs are usually very time-consuming, a disadvantage common to all genetic algorithms. More recently, a modified touring ant colony optimization (MTACO) algorithm was used in null steering [8] and seems to be faster than GAs for null-steering problems.

On the other hand, the differential evolution (DE) algorithm has been gaining acceptance recently, and has already been applied to solve many challenging engineering problems, such as electromagnetic inverse scattering [9–11] and magnetic bearings design [12]. However, DE has rarely been applied in the area of antennas. We have proposed the use of DE for the suppression of sidebands in time-modulated antenna

Correspondence to: S. W. Yang; email: TSLYSW@nus.edu.sg.
Published online in Wiley InterScience (www.interscience.wiley.com). DOI 10.1002/mmce.10118

arrays [13], which is the first application of DE to antennas that we are aware of. DE can be used to overcome most of the drawbacks in GAs [9], and has the following advantages. Firstly, DE gives all parent individuals equal chance to generate the next generation, and there is no discrimination against the less fit individuals. Secondly, the mutation is conducted by mutating the parents with population-derived difference vectors, at the beginning of each evolution loop. Thus, the destructive mutation in GAs can be avoided. Finally, the competition between individual parent and individual child takes place after crossover. Consequently, all individuals in the current generation are as good as or better than those in the previous generation.

In this article, the DE algorithm is employed to synthesize array-pattern nulling by controlling the excitation only amplitudes. The DE-simulated results are also compared with those optimized by MTACO in [8] and that by the standard binary-coded GA (SGA) in [6]. Several examples are used to demonstrate the advantages of DE over the widely used GA array pattern-nulling synthesis.

II. PROBLEM STATEMENT

Consider a symmetric linear array of $2N$ uniformly spaced isotropic elements which are controlled by amplitude only, with the array broadside far-field pattern given by

$$E(\theta) = 2\sum_{k=1}^{N} A_k \cos\left(\frac{2\pi d}{\lambda}\sin\theta\right), \qquad (1)$$

where d is the inter-element spacing, θ is the angle measured from broadside directions, and A_k is the excitation amplitude for each element.

The essence of array-pattern synthesis with prescribed nulls is to determine the optimum vector $v = \{A_k\}$ whose far-field patterns satisfy the required null positions, null depth and null width, or even with prescribed SLLs. Therefore, the array-nulling synthesis problem can be cast into an optimization problem in which a global optimization method (for example, GA, MTACO, or DE) can be utilized. Generally, the fitness or cost function description is a very critical consideration when using global optimization methods. For amplitude-only array pattern nulling synthesis, the cost function can be selected as

$$f^{(n)}(\mathbf{v}) = \sqrt{\sum_{i=1}^{M} w_i\left|E_i^{(n)}(\mathbf{v}) - NLD_i\right|^2 + w_{M+1}\cdot\left|SLL_{\max}^{(n)}(\mathbf{v})\right|^2}, \qquad (2)$$

where n stands for the number of evolution generations, M is the total number of specified elevation angles of interference sources, NLD_i is the desired null depth level for the i^{th} interference source, $SLL_{\max}$ is the calculated maximum SLL, and w_i ($i = 1, 2, \ldots, M{+}1$) is the weight factors of each term. Instead of adding another term in the cost function to control the dynamic range ratio of the element excitations [8], here, the excitation dynamic range ratio is directly controlled by setting the search ranges of the variables A_k ($k = 1,2,\ldots,N$). The weight factors w_i ($i = 1,2,\ldots,M + 1$) is set to 0 if the corresponding $E_i^{(n)} \leq NLD_i$ or $SLL_{\max}^{(n)} \leq SLL_D$ (SLL_D is the desired maximum SLL). All field quantities in eq. (2) are in amplitude instead of dB.

III. DIFFERENTIAL EVOLUTION ALGORITHM

As in the case with GAs, the DE algorithm also belongs to a broad class of evolutionary algorithms [14]. Following the procedures described in [9–11, 14], a detailed flowchart of the DE algorithm is shown in Figure 1. As can be seen, DE operates on a population with N_{POP} individuals, and each individual is a symbolic representation of the vector consisting of the N_{PAR} optimization parameters. Moreover, DE also operates using the three kinds of operators: mutation, crossover, and selection; however, these are quite different from those in GAs.

The mutation takes place first, and the mutant vector $\mathbf{v}^{M,i}$ can be generated according to

$$\mathbf{v}^{M,i} = \mathbf{v}^{(n),opt} + \beta(\mathbf{v}^{(n),p_1} - \mathbf{v}^{(n),p_2}), \quad i \neq p_1 \text{ and } i \neq p_2, \qquad (3)$$

where n is the generation index, i, p_1, and p_2 are three randomly selected individual indices in the parent population, and the superscript *opt* refers to the optimal individual in the population. The real constant β is the mutation factor. There are some other forms of mutation schemes available [14]. Occasionally, some genes (here, the optimization parameters) of the mutant vector may exceed their search ranges. Although some degree of freedom may be given such that the

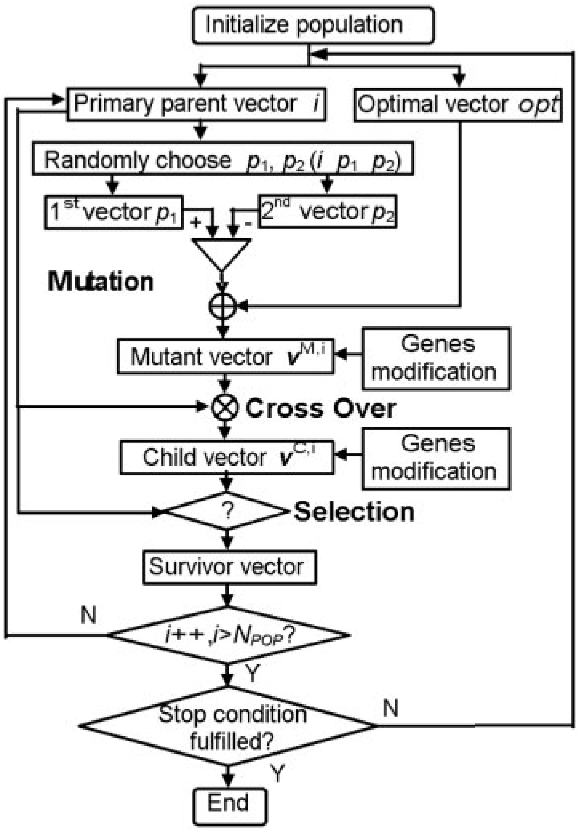

Figure 1. Overall flowchart of the DE algorithm.

DE algorithm will find the correct solution when the search ranges are set incorrectly, this will be harmful to the convergence, and thus needs to be corrected. One way to correct these foul genes is given by

$$(v^{M,i})_j = \begin{cases} \dfrac{(v^{M,i})_j + B^i}{2}, & (v^{M,i})_j < A^i \\ \dfrac{(v^{M,i})_j + A^i}{2}, & (v^{M,i})_j > B^i \end{cases}, \tag{4}$$

where j is the gene index, and $\lfloor A^i, B^i \rfloor$ is the search range of the i^{th} optimization parameter.

After mutation, the mutant vector is then mated (via crossover) with its corresponding parent vector to generate the child vector, according to

$$(\boldsymbol{v}^{C,i})_j = \begin{cases} (\boldsymbol{v}^{M,i})_j, & \gamma \le p_{cross} \\ (\boldsymbol{v}^{(n),i})_j, & \text{otherwise} \end{cases}, \tag{5}$$

where the superscript C means children population, γ is a real random number in the range [0,1], and the real constant p_{cross} is the probability of crossover. Moreover, if any genes of the child vector do not inherit from the mutant vector (which means no evolution happens), they will be modified accordingly.

Finally, the child vector and its corresponding parent vector compete for the right to survive in the next generation, depending upon who has the lower cost function value. The complete iteration procedure shown in Figure 1 indicates that DE is much simpler than GAs, and its fast convergence and strong search ability will be justified in the following linear array pattern nulling synthesis examples.

IV. NUMERICAL RESULTS

In order to evaluate the performance of the proposed DE algorithm, this section presents the numerical results calculated by DE in comparison with other methods, such as the GA and MTACO. For comparison, a linear array of 20 isotropic elements at half-wavelength spacing is considered. The array excitation amplitude is symmetric ($N_{PAR} = 15$) and the far-field patterns with single, multiple, and broad nulls in the prescribed directions are to be synthesized by the DE algorithm. Typical DE-simulation parameters are set as follows: $N_{POP} = 5N_{PAR}$, $\beta = 0.6$, $p_{cross} = 0.9$. For comparison purposes, some of the examples are also simulated by the real-coded GA (RGA) method [15], which was shown to be superior to the SGA for real parameter problems [15]. The RGA simulation parameters are chosen as: $N_{POP} = 200$, $p_{cross} = 0.8$, and $p_{mut} = 0.1$.

In the first example, the array pattern with a single null at 14° and a constrained excitation dynamic range ratio of 3.95 is considered. This example was calculated using MTACO [8] (see Fig. 4 in [8]). We do not have a MTACO code; however, the excitations optimized by MTACO were given in Table 1 in [8]. The excitation dynamic range ratio for our DE simulation was chosen as 1:0.254, which is the same as that of Fig. 4 in [8]. For DE and RGA simulation, the desired maximum SLL and the desired null depth were chosen according to the MTACO simulated results of −28.2 dB and −130.5 dB. Figure 2 shows the comparison of the far-field patterns among the DE-simulated results, the RGA-simulated results, and the MTACO-simulated results in [8]. As can be seen, all of the three simulation results agree well on the null positions, null depth, and SLLs. The actual DE- and RGA-simulated SLLs/null depths are −28.3 dB/−138.8 dB, and −28.3 dB/−133.9 dB, respectively. Typical convergence performances of the DE and RGA simulations are compared in Figure 3, in which DE converges much faster than RGA, with only about 1/3 of the generations used in RGA sim-

TABLE I. DE-Optimized Element Excitation Amplitudes for Figs. 2, 4–7

	Excitation Amplitudes				
Element Numbers	Figure 2	Figure 4	Figure 5	Figure 6	Figure 7
1, 20	0.286	0.252	0.243	0.205	1.0
2, 19	0.274	0.245	0.259	0.207	2.643
3, 18	0.329	0.322	0.477	0.352	4.255
4, 17	0.492	0.459	0.531	0.435	6.152
5, 16	0.638	0.627	0.602	0.578	8.223
6, 15	0.798	0.735	0.642	0.723	10.277
7, 14	0.844	0.877	0.866	0.800	12.174
8, 13	0.988	0.935	0.951	0.936	13.781
9, 12	0.970	0.989	0.919	1.0	14.943
10, 11	1.0	1.0	1.0	0.932	15.534

ulation. In terms of the overall computational complexity, which can be defined as the product of N_{POP} and the total number of iterations, DE has much less computational complexity than RGA.

For the simulation speed comparison between DE and MTACO [8], the MTACO simulation takes about 4–7 min on a Pentium III 750-MHz PC [8]. The DE simulation of the previous example only takes about 1–3 min on an older Intel Pentium 300-MHz PC, and takes less than 1 min on a Pentium III 1.6-GHz PC. Obviously, the DE simulation is also much faster than MTACO for array-pattern nulling.

The second example is based on Fig. 6 in [8], in which the array pattern has a null at 14° and a constrained SLL < -30 dB. The excitation dynamic range ratio for the DE simulation is the same as that used in MTACO [8], that is, 1:0.230. Figure 4 shows the DE-simulated far-field patterns in comparison with the MTACO simulated results in [8]. As can be seen, the actual DE-simulated SLL/null depth are -30.4 dB/-143.1 dB, which are better than the MTACO results of -28.2 dB/-130.5 dB. The DE simulation times are also less than 1 min on a Pentium III 1.6-GHz PC.

The third example is based on Fig. 7 of [8], in which the array pattern has a broad null sector centered at 30° with $\Delta\ \theta = 5°$. The search range for the DE simulation is the same as that used in MTACO [8], that is, 1:0.230. Figure 5 plots the DE-simulated array pattern. As compared with the MTACO results, the DE-simulated pattern obtains the same spatial range of about 5° centered at 30° for a null depth of -64 dB, while maintaining the same SLL as that of MTACO (-27 dB).

The fourth example is based on Fig. 9 of [8], in which three nulls are imposed at 14°, 25°, and 40°. Again, the search range for the DE simulation (1:

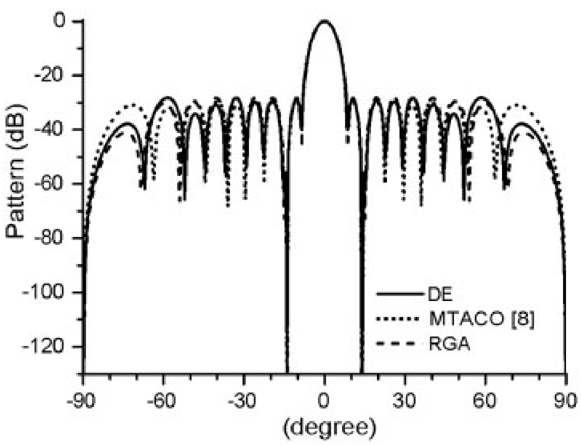

Figure 2. Comparison of the radiation patterns with one null imposed at 14° among the results optimized by DE (solid line), MTACO (dotted line), and RGA (dashed line). Amplitude search range: 1:0.254.

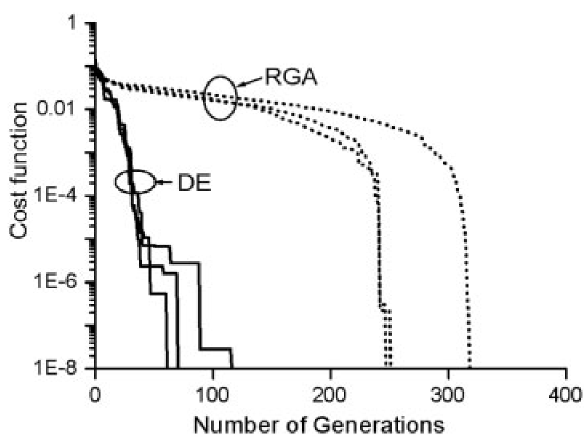

Figure 3. Comparison of the convergence performance between the DE algorithm (solid lines) and RGA (dotted lines).

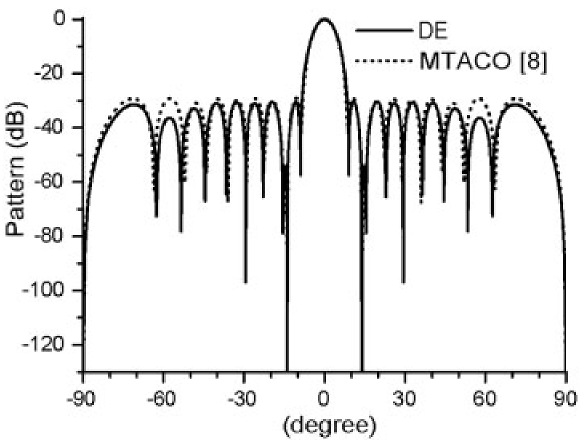

Figure 4. DE-optimized radiation pattern (solid line) with one null imposed at 14° in comparison with the result by MTACO (dotted line). Amplitude search range: 1:0.230.

0.202) is the same as that used in MTACO [8]. The comparison between the DE-optimized array pattern and the MTACO optimized pattern is shown in Figure 6. It is observed that the DE-optimized results are better than the MTACO results, as the DE-optimized pattern has a maximum SLL of −30 dB, with all desired nulls lower than −90 dB.

Finally, the example based on Fig. 5 in [6] is considered. This example synthesizes the 20-element array pattern with nulls at nine interference directions, respectively coming from the peak sidelobes of the initial −30-dB SLL Chebyshev pattern, namely, at 10°, 14.5°, 20°, 26°, 32.5°, 40°, 48°, 58°, and 71.5° [6]. The target is: $SLL_D \leq -30$ dB, and $NLD_i \leq -60$ dB ($i = 1, \ldots, 9$). The DE search range for the current amplitude is selected to be the same as that of [6], i.e.,

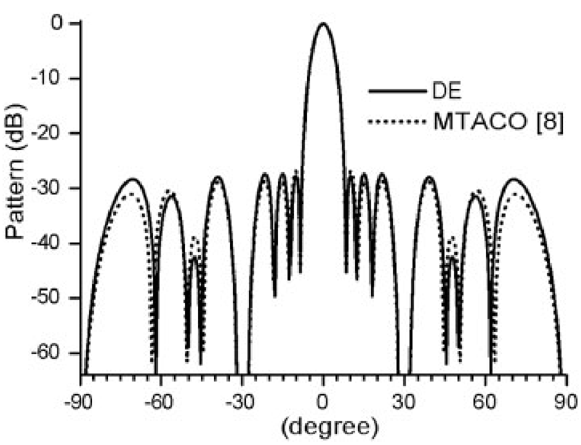

Figure 5. DE-optimized radiation pattern (solid line) with a broad null ($\Delta\theta = 5°$) centered at 14° compared with the result by MTACO (dotted line). Amplitude search range: 1:0.230.

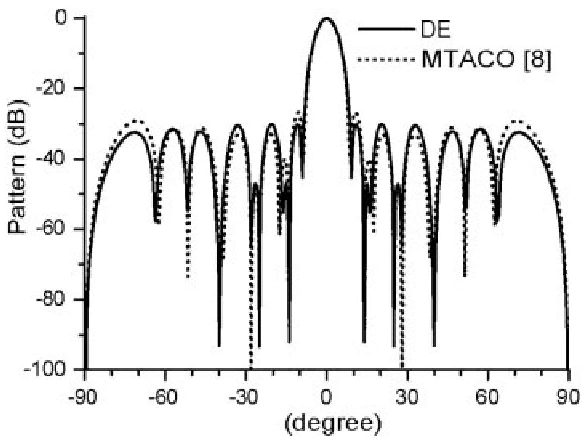

Figure 6. DE-optimized radiation pattern (solid line) with three nulls imposed at 14°, 25°, and 40°, compared with the result by MTACO (dotted line). Amplitude search range: 1:0.202.

1:15.549. Figure 7 shows the array pattern comparison among the DE optimized result, the RGA optimized result and the SGA optimized result in [6]. As can be seen, the DE optimized pattern can satisfy the more stringent target of $SLL_D \leq -30$ dB and $NLD_i \leq -65$ dB ($i = 1,\ldots,9$), while the RGA and SGA results cannot meet the requirements of null depth below −60 dB at most of the nine interference directions. This example clearly demonstrates the strong search ability of the DE algorithm over the RGA and SGA. Figure 8 plots a comparison of the typical convergence performances by the DE and RGA simulations for this problem. It is observed that DE usually converges at about 100 generations, while RGA cannot converge with 10000 generations.

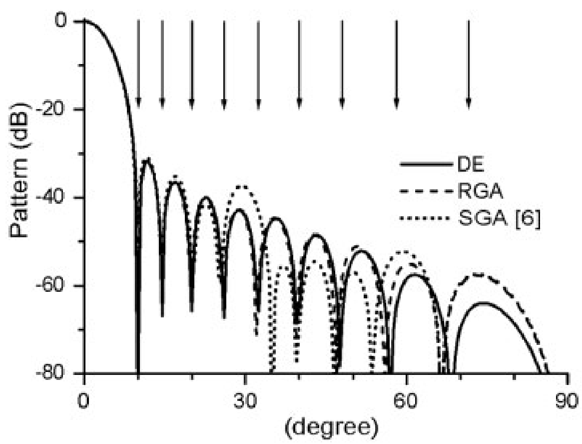

Figure 7. DE-optimized radiation pattern (solid line) with nine nulls imposed at the peaks of a −30-dB SLL Chebyshev pattern, compared with the result by SGA (dotted line). Amplitude search range: 1:15.549.

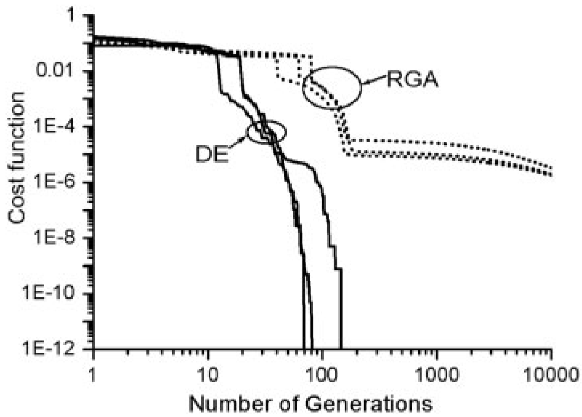

Figure 8. Comparison of the convergence performance between the DE algorithm (solid lines) and RGA (dotted lines).

For verification purposes, the DE-optimized element excitation amplitudes for Figures 2, 4–7 are summarized in Table I. Taking possible practical implementations into consideration, the DE-optimized amplitudes are truncated to three-digit accuracy only. Note that the DE-optimized amplitudes are within the search ranges of the respective examples cited from [6] and [8]. The amplitudes for Figures 2, 4–6 are normalized with respect to their respective maximum values, while the amplitudes for Figure 7 are normalized with respect to those of the edge elements.

V. CONCLUSION

A numerical approach based on the DE algorithm has been proposed for efficient of antenna-array pattern synthesis with prescribed nulls at the directions of interferences, by controlling only the array element excitation amplitudes. Numerical results in comparison with the published data have illustrated distinct features of the DE algorithm over other algorithms such as MTACO and GA, especially with regard to search ability, robustness, fast convergence, and so on. Although only linear antenna arrays have been considered here, the DE algorithm can be applied to arrays with complex geometry as well as nonisotropic elements.

REFERENCES

1. R.L. Haupt, Adaptive nulling in monopulse antennas, IEEE Trans Antennas Propagat AP-36 (1988), 202–208.
2. M.J. Mismar and T.H. Ismail, Null steering using the minimax approximation by controlling only the current amplitudes, Int J Electron 78 (1995), 409–415.
3. R.L. Haupt, Phase-only adaptive nulling with a genetic algorithm, IEEE Trans Antennas Propag, AP-45 (1997), 1009–1015.
4. W.P. Liao and F.L. Chu, Null steering in planar arrays by controlling only current amplitudes using genetic algorithm, Microwave Opt Technol Lett 16 (1997), 97–103.
5. W.P. Liao and F.L. Chu, Array pattern nulling by phase and position perturbations with the use of the genetic algorithm, Microwave Opt Technol Lett 15 (1997), 251–256.
6. W.P. Liao and F.L. Chu, Array pattern synthesis with null steering using genetic algorithms by controlling only the current amplitudes, Int J Electron 86 (1999), 445–457.
7. Y.C. Chung and R.L. Haupt, Amplitude and phase adaptive nulling with a genetic algorithm, J Electromagn Waves Applic 14 (2000), 631–649.
8. N. Karaboga, K. Güney, and A. Akdagli, Null steering of linear antenna arrays with use of modified touring ant colony optimization algorithm, Int J RF Microwave Computer Aided Eng 12 (2002), 375–383.
9. A. Qing, Electromagnetic inverse scattering of multiple two-dimensional perfectly conducting objects by the differential evolution strategy, IEEE Trans Antennas Propag AP-51 (2003), 1251–1262.
10. K.A. Michalski, Electromagnetic imaging of circular-cylindrical conductors and tunnels using a differential evolution algorithm, Microwave Opt Technol Lett 27 (2000), 330–334.
11. K.A. Michalski, Electromagnetic imaging of elliptical-cylindrical conductors and tunnels using a differential evolution algorithm, Microwave Opt Technol Lett 28 (2001), 164–169.
12. G. Stumberger, D. Dolinar, U. Palmer, and K. Hameyer, Optimization of radial active magnetic bearings using the finite element technique and the differential evolution algorithm, IEEE Trans Magnet 36 (2002), 1009–1013.
13. S. Yang, Y.B. Gan, and A. Qing, Sideband suppression in time modulated linear arrays by the differential evolution algorithm, IEEE Antennas Wireless Propag Lett 1 (2002). 173–175.
14. R. Storn and K. Price, Differential evolution — A simple and efficient heuristic for global optimization over continuous spaces, J Global Optimization 11 (1997), 341–359.
15. A. Qing, C.K. Lee, and L. Jen, Electromagnetic inverse scattering of two-dimensional perfectly conducting objects by real-coded genetic algorithm, IEEE Trans Geosci Remote Sensing 39 (2001), 665–676.

BIOGRAPHIES

Shiwen Yang received his B.Sc. degree in electronic science from East China Normal University, Shanghai, China, his M.Eng. degree in electromagnetics and microwave technology and Ph.D. degree in physical electronics from the University of Electronic Science and Technology of China (UESTC), Chengdu, China, in 1989, 1992, and 1998, respectively. From 1992 to 1998, he worked as a Lecturer at the Institute of High Energy Electronics, UESTC. From 1998 to 2001, he was a Research Fellow at the School of Electrical and Electronic Engineering, Nanyang Technological University, Singapore. He is currently a Research Scientist at Temasek Laboratories, National University of Singapore. His research interests include antennas and arrays, evolution algorithms, computational electromagnetics, and high-power microwaves.

Yeow-Beng Gan received his M.Eng and B.Eng (Hons) degrees in electrical engineering from the National University of Singapore, in 1994 and 1989, respectively. He has been with the DSO National Laboratories (formerly the Defence Science Organization) since 1989. He was the founding member of the antenna group in DSO, and was responsible for building up the technical capabilities in the area of antenna analysis and design. He became a Principal Member of Technical Staff in 1998. In May 2001, he was seconded to Temasek Laboratories, National University of Singapore, where he is currently a Principal Research Scientist. His research interests include periodic arrays for antennas and radomes, wave physics, computational electromagnetics, and modeling of composite materials. He is a Senior Member of IEEE.

Anyong Qing was born in Hu'nan province, P. R. China, in 1972. He received his B.E. degree from Tsinghua University in 1993, M.E. degree from Beijing Broadcasting Institute in 1995, and Ph.D. degree from Southwest Jiaotong University in 1997, all majoring in electromagnetic theory and microwave technology. His research interests include composite materials, electromagnetic, acoustic and elastic waves scattering and propagation, electromagnetic/acoustic inverse scattering, frequency-selective surfaces, and genetic algorithms. He was a postdoctoral fellow in the Department of Communication Engineering, Shanghai University, during September 1997 and June 1998, and a research fellow in the School of Electrical and Electronic Engineering, Nanyang Technological University, Singapore. He was a Member of Scientific Staff in the Electromagnetic Theory Group at the Department of Electrical Engineering, University of Kassel, Germany, during July 2000 and May 2001. He joined VS Electronics Pte.. Ltd., Singapore, as an RF Design Engineer in June 2001 and was jointly with Sumitomo Electric Industries Ltd, Itami, Japan. He is currently a Research Scientist with Temasek Laboratories, National University of Singapore. He serves as reviewer for *IEEE Transactions on Antennas and Propagation*, *IEEE Transactions on Geoscience and Remote Sensing*, *IEEE Antennas and Wireless Propagation Letters*, *Inverse Problems*, and *Journal of Electromagnetic Waves and Applications*.

He is a member of the IEEE and Chinese Institute of Electronics.